

Potent antimicrobial small molecules screened as inhibitors of tyrosine recombinases and Holliday junction-resolving enzymes

Marc C. Rideout · Jeffrey L. Boldt · Gabriel Vahi-Ferguson · Peter Salamon · Adel Nefzi · John M. Ostresh · Marc Giulianotti · Clemencia Pinilla · Anca M. Segall

Received: 29 January 2011 / Accepted: 30 August 2011
© Springer Science+Business Media B.V. 2011

Abstract Holliday junctions (HJs) are critical intermediates in many recombination-dependent DNA repair pathways. Our lab has previously identified several hexameric peptides that target HJ intermediates formed in DNA recombination reactions. One of the most potent peptides, WRWYCR, is active as a homodimer and has shown bactericidal activity partly because of its ability to interfere with DNA repair proteins that act upon HJs. To increase the possibility of developing a therapeutic targeting DNA repair, we searched for small molecule inhibitors that were functional surrogates of the peptides. Initial screens of heterocyclic small molecule libraries resulted in the identification of sev-

eral *N*-methyl aminocyclic thiourea inhibitors. Like the peptides, these inhibitors trapped HJs formed during recombination reactions in vitro, but were less potent than the peptides in biochemical assays and had little antibacterial activity. In this study, we describe the screening of a second set of libraries containing somewhat larger and more symmetrical scaffolds in an effort to mimic the symmetry of a WRWYCR homodimer and its target. From this screen, we identified several pyrrolidine bis-cyclic guanidine inhibitors that also interfere with processing of HJs in vitro and are potent inhibitors of Gram-negative and especially Gram-positive bacterial growth. These molecules are proof-of-principle of a class of compounds with novel activities, which may in the future be developed into a new class of antibiotics that will expand the available choices for therapy against drug-resistant bacteria.

Electronic supplementary material The online version of this article (doi:10.1007/s11030-011-9333-2) contains supplementary material, which is available to authorized users.

The first two authors should be considered co-first authors.

M. C. Rideout · J. L. Boldt · G. Vahi-Ferguson · A. M. Segall (✉)
Department of Biology and Center for Microbial Sciences,
San Diego State University, San Diego, CA 92182, USA
e-mail: aseball@sciences.sdsu.edu

Present Address:

J. L. Boldt
Genomatica, Inc., 10520 Wateridge Circle, San Diego, CA 92121,
USA

G. Vahi-Ferguson · P. Salamon
Department of Mathematics and Statistics, San Diego State
University, San Diego, CA 92182, USA

A. Nefzi · M. Giulianotti
Torrey Pines Institute for Molecular Studies, 11350 SW Village
Parkway, Port St. Lucie, FL 34987-2352, USA

J. M. Ostresh · C. Pinilla
Torrey Pines Institute for Molecular Studies, 3550 General Atomics
Court, 2-129, San Diego, CA 92121-1120, USA

Keywords Site-specific recombination · λ -Integrase · Holliday junction · Combinatorial libraries · DNA repair

Introduction

Site-specific recombination (SSR) catalyzed by phage λ Integrase (Int) and enzymes belonging to the tyrosine recombinase family requires the formation and subsequent resolution of a Holliday junction (HJ) intermediate (Fig. 1a). These enzymes are widespread, and include a subclass of bacterial-encoded enzymes, for example, XerC and XerD of *E. coli* and RipX and CodV of *B. subtilis*, which help in the process of segregation of chromosomes to daughter cells. The mechanism and structure of these enzymes has been extensively studied [1]. Previously, hexapeptide inhibitors that trapped recombinase-bound HJ intermediates and blocked recombination were isolated by screening and deconvoluting synthetic peptide combinatorial libraries [2–5]. Further analysis

of the most potent peptide WRWYCR (Fig. 1b) showed that its activity required the formation of a dodecapeptide via a disulfide bridge between the cysteines from each of the two hexapeptides [4]. Peptides that do not readily dimerize were also identified in the screen (e.g., WKHYNY, Fig. 1c) but homodimers of WRWYCR or KWWCRW were more effective at trapping HJs in vitro and in vivo [6–9].

The activities of WRWYCR and KWWCRW are not dependent on interactions with any of the tyrosine recombinase proteins, which are very diverse in their primary amino acid sequence [4,8,11]. WRWYCR and KWWCRW also inhibit DNA cleavage and HJ resolution by Vaccinia virus topoisomerase, the prototype of type IB topoisomerases [3, 12]. The mechanisms and structures of the catalytic domains of tyrosine recombinases and type IB topoisomerases are highly related [13, 14]. In addition, these peptides also inhibit structurally and mechanistically unrelated HJ-processing enzymes, like RecG helicase and RuvABC resolvase, which share with the tyrosine recombinases only their interactions with HJs [9]. The activities of the peptides are based on their ability to bind to the open or square planar conformation [15] of the protein-free HJs, and with lesser affinity to other branched DNAs, including replication forks [9].

HJs are central intermediates in several DNA repair pathways that are required during bacterial growth, and particularly in environments in which bacteria experience DNA damage, such as the immune system of mammalian hosts [16–18]. WRWYCR, KWWCRW, and their D-amino acid stereoisomers, wrwycr and kwwcrw, are broad spectrum antibacterials that have minimal inhibitory concentrations (MIC) values ranging from 32 to 64 $\mu\text{g}/\text{mL}$ in Gram-negative bacteria and 4 to 32 $\mu\text{g}/\text{mL}$ in Gram-positive bacteria [8]. While bacteria recover from treatment with even high doses of the L-amino acid isomers, they recover less or not at all from the D-amino acid peptides. The peptides are bactericidal, and their effect is synergistic with other DNA-damaging agents, including UV, mitomycin C, H_2O_2 , and norfloxacin in bacteria or etoposide in HeLa and U2OS cells [8] (I. Naili et al., unpublished data; L. Su et al., unpublished data). This hypothesis led us to propose that the need for DNA repair creates HJ targets for the peptides, blocking further repair and/or DNA synthesis and causing the accumulation of fragmented DNA and ultimately cell death [8] (Y. Xu et al., unpublished data; C. Gunderson and A. Segall, unpublished data). Peptide wrwycr has antibacterial activity against *Salmonella enterica* serovar Typhimurium in murine macrophage cells, and the treatment of *Salmonella*-invaded J774A.1 macrophages with wrwycr induces the SOS response in the intracellular bacteria [19].

DNA repair intermediates such as HJs are largely unexploited antibacterial targets, and resistance is less likely to develop because HJs are generated in multiple independent ways [16]. Indeed, we have been unable to isolate stable

peptide-resistant mutants. In light of the emergence of multiple drug resistance in bacteria, we have been investigating the possibility of developing these inhibitors into therapeutic agents. Peptide-based drugs have some disadvantages. We have overcome a major disadvantage of the sensitivity of L-amino acid peptides to proteolysis by means of the D-isomer version of the same peptides [4,7,8]. Other disadvantages of peptides are relatively high molecular weights, which lead to poor bioavailability and permeability across the intestinal and blood–brain barriers [20]. Moreover, peptides may have an excess of hydrogen bond donors and acceptors, often considered negative characteristics for potential therapeutics [21].

In order to find non-peptide compounds with similar activities, we performed screens of small molecule libraries to isolate HJ-trapping surrogates. The diversity of the mixture-based small molecule libraries is derived, as in the case of the peptide libraries, from functional groups (analogous to peptide R groups) on a unique scaffold [22–25]. Our initial small molecule screen focused on libraries built on scaffolds with low molecular weight, and yielded a *N*-methyl aminocyclic thiourea that traps HJs formed during SSR reactions in vitro (1530-1, Fig. 1d and Ref. [26]). This inhibitor binds specifically to protein-free HJs and inhibits HJ resolution by RecG. While showing that the same strategy that yielded potent peptide inhibitors could also yield non-peptide molecules with analogous activities, 1530-1 is less potent in in vitro reactions and showed only about 50% growth inhibition of a hyperpermeable *Salmonella* strain at 128 $\mu\text{g}/\text{mL}$ [18]. A major difference between the most potent hexapeptide inhibitors and 1530-1 is a relatively low potential for forming dimers (Fig. 1b, d). In order to identify more potent compounds with antibacterial activity, we repeated the screen focusing specifically on libraries built on larger, more symmetric scaffolds in an effort to mimic the most potent peptide homodimers. In this article, we describe the identification of several pyrrolidine bis-cyclic guanidine inhibitors that inhibit phage lambda SSR and trap HJs. These compounds recognize protein-free HJs, inhibit HJ resolution by RecG helicase, and have antibacterial activity at least as potent as the peptides wrwycr and kwwcrw.

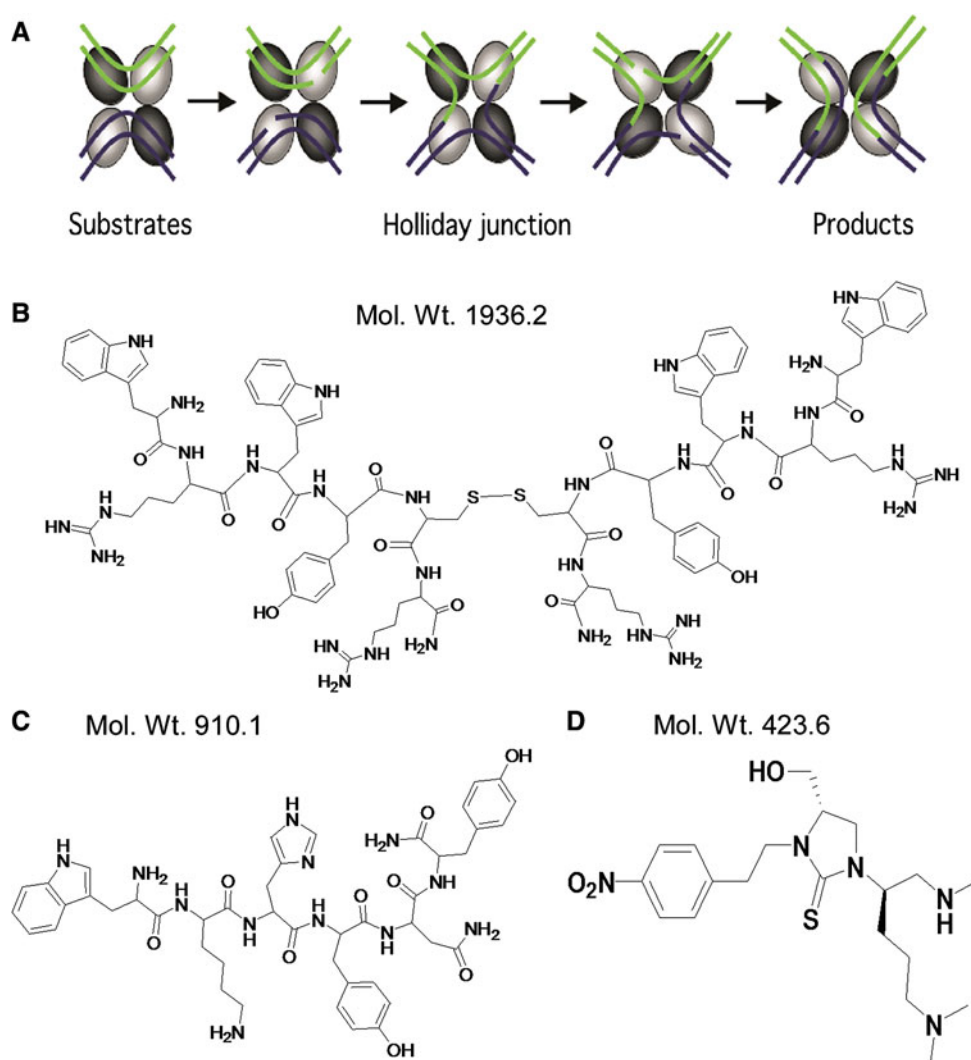
Experimental section

Chemistry

Libraries and compound synthesis

The mixture-based libraries that were screened were synthesized at Torrey Pines Institute for Molecular Studies (TPIMS). Based on the results of the screens, individual small molecules were selected for synthesis, which was also

Fig. 1 Inhibitors of Int-mediated recombination. **a** Schematic of the tyrosine recombinase-mediated SSR pathway. Four Int monomers synapse the recombining DNA molecules; only the regions around the site of strand exchange are shown. Two Int monomers (shown as *light grey ovals*) each cleave opposing strands of DNA to form a covalent protein–DNA adduct at the 3' end, leaving a free 5' OH group. The strands ending in the 5' OH groups are exchanged and ligated, forming the HJ intermediate. In the absence of any inhibitors, the second pair of Int monomers cut, exchange, and religate the second pair of DNA strands, resolving the HJ into recombinant products. The HJ is the primary target of the inhibitors, preventing cleavage of either pair of DNA strands. The requirement for the accessory proteins IHF and Xis (not shown) are dependent on the specific recombination pathway [10]. **b** Structure of a WRWYCR dimer. **c** Structure of WKHYNY. **d** Structure of *N*-methyl aminocyclic thiourea, 1530-1



performed at TPIMS as described [24]. All reagents for the synthesis were purchased from commercial suppliers, and were used without further purification. Individual compounds identified from the screens were synthesized in parallel in 100-mg “tea bags” using methylbenzylhydramine (MBHA) resin as a support. Compounds were cleaved from the support using HF, extracted from the tea bags with 95% acetic acid and sonication for 10 min and lyophilized to yield between 80 and 95 mg of crude compound. Samples were dissolved at a concentration of 1.0 mg/mL in 50% acetonitrile in water (ACN/water) and a 20- μ L aliquot was injected onto a C-18 column on a Finnegan LC-MS system (Finnegan HPLC equipped with a Finnegan Surveyor photodiode array detector (PDA) and a Finnegan LCQ duo Mass Spectrophotometer). All the solvents for liquid chromatography contained 0.05% TFA as a buffer. Compounds were eluted from the column using a gradient from 5% (ACN/water) to 95% (ACN/water) over 6 min with a flow rate of 250 μ L/min. The presence of the preferred compounds was confirmed by their

mass, and the purity of the crude material was determined to be 70–80% as judged by UV absorption at 254 nm. A small amount of the crude compounds was resuspended in 10–50% (DMSO/water) and screened in the indicated biological assays without further purification.

Small molecule purification

Pyrrolidine bis-cyclic guanidine compounds (1609: 1, 3, 10, and 12) were purified as follows. Each crude compound was initially solubilized in 2 mL of 50% (ACN/water) and then diluted to 10% (ACN/water), causing a precipitate to form. Concentrated HCl (2.5%, v/v) was added and the compounds were sonicated for 5 min to help solubilize them. A 20- μ L aliquot of each compound solution was injected onto the Finnegan LC-MS. The product with the required molecular weight was identified and, based on its retention time, a unique gradient was created for the purification of each molecule. The crude compounds were purified on an Agilent 1100

HPLC with a semi-prep C18 column using the established gradient and an initial mobile phase of 10% (ACN/water) with a flow rate of 10 mL/min. In general, peak fractions eluted between 45 and 75% (ACN/water). Ten 1-mL fractions were collected, and each was screened by LC-MS to confirm the purity and correct molecular weight. Fractions were pooled, lyophilized, resuspended in 50% (DMSO/water), and stored at 4 °C. An aliquot of the purified material for each compound was analyzed on a Beckman HPLC (Model 128 pump with a model 168 photo diode array detector) and a Phenomenex Jupiter 4 μ m Proteo 90Å (250 \times 4.6 mm) C8 analytical column. The purity of each compound was determined to be 90–95% (compounds 1609-1, 3, and 12) and 82% for 1609-10. Final yields for each purified compound were between 5 and 10 mg. High-resolution mass spectrometry was performed for the four purified compounds. These data can be found in Online Resource 1 (OR 1).

Biological assays

All acrylamide gels used in this study were made from 29:1 polyacrylamide:bis-acrylamide solutions. Oligonucleotides were purchased from Integrated DNA Technologies and, in the case of oligos used directly as reaction substrates, were purified on 5% native polyacrylamide gels. DNA was visualized by “UV shadowing” using a hand-held Mineral lamp, model UVGL-58 (366 nm), and the correct molecular weight product was excised from the gel and eluted using a “crush/soak” method [27]. DNA oligomers were precipitated and resuspended at the indicated concentrations for use in PCR, or were directly annealed together to make HJ substrates. DNA substrates were radiolabeled using [γ -³²P]-ATP (Perkin Elmer, BLU-502Z) and T4 polynucleotide kinase (New England Biolabs, NEB), as described previously [4]. Gels were dried on a gel dryer at 80 °C under vacuum for 2 h. Dried gels were exposed to a molecular dynamics (MD) PhosphorImager screen, and quantitated with ImageQuant software from MD.

Excision recombination assays

The excision assays were performed using the same DNA substrates, and exactly as described in [4].

Bent-L recombination assays

The bent-L assays were performed using the same DNA substrates, and exactly as described in [4].

RecG helicase assays

RecG unwinding assays were performed as described previously [9], using the same oligonucleotides as substrates.

RecG was the generous gift of Dr. Peter McGlynn (University of Aberdeen).

Restriction enzyme inhibition

pUC19 DNA was purified from RecA⁻ cells. The amount of *Hind*III restriction enzyme (New England Biolabs) was first titrated in reactions containing 43.2 ng plasmid DNA to establish conditions where 50–70% of the total input DNA was cut after 25 min at 37 °C with 0.08 units of *Hind*III per reaction. To examine inhibition, purified small molecules were added to reactions at the indicated concentrations and incubated 10 min at 37 °C. Reactions were then started with the addition of restriction enzyme, and aliquots were taken at either 2, 5, 15, or 25 min, and stopped with 2% SDS, 10% glycerol, and 0.1% bromophenol blue. Reactions were electrophoresed on 0.7% agarose gels with a final concentration of 2.5 μ g/mL ethidium bromide, at 5 V/cm and 0.5 \times TBE. The DNA was visualized on a GeneFlash gel documentation system (Imgen Technologies) with UV exposure at 258 nm. The image was quantitated for % DNA cleavage using ImageQuant (GE Lifesciences) software.

Electrophoretic mobility shift assay (EMSA)

The following oligos were used for assembling a junction with symmetrical arms and a frozen center that cannot branch migrate (oligos shown 5' to 3'):

1. TCCTACCACCAGATACACGCCACAG
TTTTTTTTTTTGATTA
2. TAATCAAAAAAAAAAACTGTGCAGA
TGCGGAGTGAAGTTCC
3. GGAACTTCACTCCGCATCTGATCTTT
GCCGTCTTGTCAA
4. TTTGACAAGACGGCAAAGATGCGT
GTATCTGGTGGTAGGGA

For these experiments, junctions were purified on an SDS–tris–tricine gel. The HJ band was excised, and eluted by the “crush/soak” method, then precipitated, and finally resuspended in 1 mM tris (pH 8.0), 0.1 mM EDTA. Binding reactions were performed with 2 nM HJ in 25 mM tris (pH 8.0), 1 mM EDTA, 100 mM NaCl, and 5% glycerol, with 100 ng of sonicated salmon sperm DNA in a 10 μ L volume. 1609-10 was allowed to incubate for 10 min on ice. Reactions were electrophoresed through a native 5% polyacrylamide gel at 4 °C with 0.5 \times TBE as running buffer. Gels were dried and analyzed as described above.

2-Aminopurine (2-AP) fluorescence binding assays

2-AP assays were performed as described previously [6] and using the same oligonucleotides as substrates. In brief, 100 nM HJ containing one 2-AP substitution of adenine, as indicated, was titrated with crude compounds at molar ratios of 0:1, 0.5:1, 1:1, 2:1, or 4:1 of small molecule:HJ. Fluorescence measurements were performed on a Photon Technology International Model QM-4/2005 scanning spectrofluorometer (Birmingham, NJ, USA). The sample was excited at 315 nm, and the fluorescence emission values obtained between 365 and 375 nm were averaged. Bandpass filters were set at 4 nm for excitation and 8 nm for emission. The averaged values were subtracted from a similar titration of a junction in which the native adenine was present in the junction, instead of 2-AP, to give corrected fluorescence (F_{corr}) values, which represent the fluorescence due to the presence of the 2-AP substitution. The F_{corr} values were then normalized to untreated reactions (shown in OR 2B). Crude compounds were initially screened using the HJ with the 2-AP site on strand four at position two (4AP2, OR 2A). Selected small molecules were screened further using three other HJs containing AP substitutions at different sites (1AP1, 3AP1, and 4AP1).

2-AP fluorescence binding of purified 1609-10 for determination of apparent dissociation constant (K_d)

Based on the initial 2AP screening and in part on *in vivo* results, purified 1609-10 was selected for extensive titration in the 2-AP assay to model the binding interactions and estimate an apparent binding constant (K_d). HJ4AP2 was used as the reporter and titrated with 1609-10 at 15 or 20 different concentrations ranging from 0 to 900 nM. F_{corr} values were determined (as described above), and then expressed as a fraction of the HJ in a complex (fraction of complex, or F_c) versus concentration of 1609-10 using the following equation:

$$F_{c_{\text{observed}}} = \frac{F_0 - F_B}{F_0 - F_S}$$

where F_0 is the initial fluorescence of the 2AP HJ, F_B is the fluorescence at a given concentration of 1609-10, and F_S is the fluorescence at saturating concentrations of 1609-10. For each titration, the saturation point was set just below the point of maximum fluorescence quenching and used to estimate an apparent K_d .

Fitting of the fluorescence data to describe the binding interactions between 1609-10 and a HJ

We modeled the predicted binding curves to the experimentally determined values, shown in Fig. 7, by testing six pos-

sible scenarios of 1609-10 binding to a HJ. These scenarios as well as the equations used in describing the best model are presented in detail in OR 3.

Stability experiments

Radiolabeled HJs were trapped in excision recombination reactions with a final concentration of 0.5 μM peptide WRWYCR. Reactions were electrophoresed on 5% SDS-tricine polyacrylamide gels, and the HJ band was cut from the gel and eluted overnight using the crush-soak method [27] in 3 volumes of TE (pH 8.0). Junction DNA was precipitated with 10% sodium acetate and 3 volumes cold ethanol, resuspended in TE and quantitated using UV. Recombination reactions were assembled as described above, using the purified junctions (20 pM final) and warmed to 30 °C before the initiation by the addition of a “pre-mix” of the recombination proteins. Reactions were allowed to proceed for 30 min, and were then diluted 20 fold with 1 \times buffers, 2 μg nonspecific DNA, and a 28-fold molar excess of unlabeled HJ over each inhibitor. Aliquots (200 L) were taken from diluted reactions at the indicated time points and stopped with 100 μL of 2% SDS. Standard reactions using the same molar amounts of DNA and proteins were assembled in either 10 or 200 μL volumes. These were used as controls to judge inhibition based on reaction volume and were quenched just before the 20-fold dilution with either 5 or 100 μL of 2% SDS, respectively. Products were separated on SDS-tricine gels, and %HJ resolution/min was calculated.

RuvABC HJ cleavage assays

Assays were performed as described previously [9] using the same oligonucleotides as substrates. We are grateful to Dr. Robert Lloyd (University of Nottingham) for his generous gifts of RuvA, RuvB, and RuvC proteins.

Minimal inhibitory concentration assays

Several bacterial strains were used to examine the inhibitory effects of the isolated small molecules. A complete strain list with genotypes can be found in OR 4. Overnight cultures were subcultured 1:100 in MHB in culture tubes and grown to an OD_{600} of 0.08–0.1. Concentrations of small molecule tested were 1, 2, 4, 8, 16, 32, 64, 128, 256, and 512 $\mu\text{g}/\text{mL}$. A 96-well plate was prepared with 2 \times desired small molecule in 100 μL of MHB. Subcultured cells (100 μL per well) were mixed into each well, and an initial OD_{600} reading of the plate was taken. Plates were incubated for 16–20 h without shaking at 37 °C, and the final OD_{600} reading was determined. The difference between the final and the initial readings was calculated to yield the increase in growth. The MIC

is defined as the lowest concentration of compound that inhibits growth [28].

MTT assays

The African green monkey kidney epithelial cell line BSC40 was seeded at 40,000 cells/well in 96-well plates, then incubated overnight at 37 °C in 5% CO₂. The medium was removed and replaced with DMEM containing the indicated treatments, and growth proceeded for 24 h. After treatment, 20 μL of 4-mg/mL 3-(4,5-dimethyl-2-thiazolyl)-2,5-diphenyl-2H-tetrazolium bromide (MTT) solution in 1 × PBS was added to each well and incubated for 3 h. Lysis buffer (100 μL of 20% SDS in water:DMF (1:1), 2% glacial acetic acid, and 2% 1M hydrochloric acid) was added and the plates were incubated overnight at 37 °C to aid the dye dispersion. Absorbance of the wells was read at OD₅₇₀ nm on a SpectraMax384 Molecular Devices microtiter plate reader. Control reactions to test the effect of DMSO (solvent for peptides and small molecules) were performed in identical fashion.

Hemolytic activity assay

Sheep's blood (MP Biomedicals) was centrifuged to separate plasma and white blood cells from the red blood cells. The red blood cells were washed 3 times in 2 mL of 1 × PBS and then resuspended to 1% in 1 × PBS. An equal volume of compounds at 2 × the test concentrations was mixed with the cells in a 96-well V-bottom plate (Costar #3894), and then incubated for 60 min at 37 °C in 5% CO₂. Distilled water was used as a positive control for hemolysis. The plate was then spun for 5 min at 1,500 rpm in a Sorval RT6000D with a H1000B rotor. Supernatant (100 μL from each well) was transferred to a clear 96-well flat bottom plate, and the optical density at 405 nm was measured using a Molecular Devices Spectramax Plus 384.

Results

The strategy used for identifying individual compounds from the combinatorial libraries is outlined in Fig. 2. Underlined text refers to specific headings in this section where more detailed explanations can be found.

Scaffold ranking

The ten mixture-based libraries screened (OR 5) were selected to have some degree of two-fold symmetry in the scaffold compared to the lead molecule 1530-1. Each of the scaffolds has functionalities, or R groups, at three or four diversity positions depending on the scaffold. These functionalities are derived from coupling L- or D-amino acids at

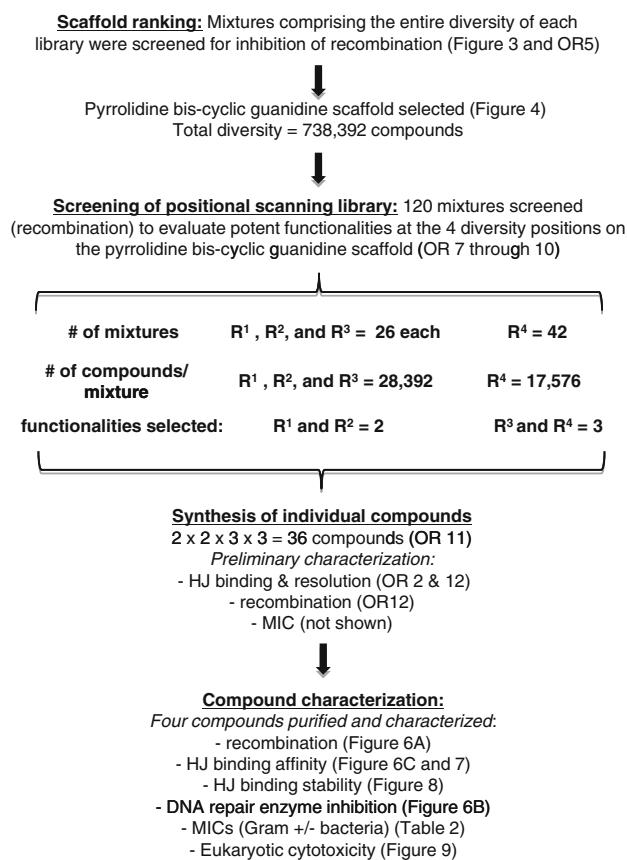


Fig. 2 Screening strategy for identification of HJ trapping small molecules from combinatorial libraries. Ten libraries were selected and screened in SSR to determine the most potent scaffold. We next screened 120 defined mixtures representing the positional scanning to determine the most potent R-group functionalities on the scaffold and the deconvolution involved the selection of the top functionalities to design 36 individual compounds, which were synthesized in parallel. After preliminary characterization, we selected four candidates for purification and further characterization in the assays listed

the first R groups, and carboxylic acids at the last R group (R³ or R⁴, depending on the scaffold). The libraries are arranged in a positional scanning format [29] composed of mixtures that can either be screened individually to identify potent R group functionalities, or pooled to test the potency of the library as a whole. For instance, the positional scanning TPI1346 library is composed of 120 mixtures ($26R^1 + 26R^2 + 26R^3 + 42R^4 = 120$) for a total diversity of 738,192 compounds ($26R^1 * 26R^2 * 26R^3 * 42R^4 = 738,192$). In mixture 1 (OR 6), every compound contains the functionality S-methyl at position R¹ and a mixture of all other possible functionalities for this library at positions R²–R⁴, yielding a total of 28,392 compounds ($1 * 26 * 26 * 42 = 28,392$). Inclusion of this mixture into a given assay allows the assessment of the functionality S-methyl at position R¹ on this scaffold. Alternatively, the 26 R¹ mixtures can be pooled, to reconstitute the entire diversity of the library, and tested similarly; the same

holds true for (R^2 , R^3 , or R^4 mixture pools). Comparisons with similar mixture pools from other libraries allows for the selection of the best library.

We tested R^1 mixture pools for each of the ten libraries in the bent-L recombination pathway (see [1] for review) at $30 \mu\text{g/mL}$. As seen in Fig. 3a, inclusion of these mixture pools leads to an increase in HJs and a concomitant decrease in recombinant products, depending on the potency of the library. We also compared these results with similar pools for the other R groups in each library (R^2 , R^3 , or R^4) and the results shown in Fig. 3b are the averages of % recombination and % HJ accumulation for all the R group pools of a given library. The relatively small error bars shown reflect the fact that each of these mixture pools does indeed represent the complete diversity of the entire library and thus they give similar results. This concept has been developed into a “scaffold-ranking strategy,” described in detail in [30].

The best-performing four libraries, TPI1276, TPI1319, TPI1345, and TPI1346, accumulated at least 25% of the input substrate as HJs (Fig. 3b). Based on a dose titration from 0.25 to $150 \mu\text{g/mL}$ of each library (Fig. 3c), we found that TPI1346 trapped the most HJs and had the lowest IC_{50} for HJ accumulation ($0.6 \mu\text{g/mL}$ vs. $2 \mu\text{g/mL}$ for the other three libraries). Library TPI1346 is synthesized on a pyrrolidine bis-cyclic guanidine scaffold (Fig. 4) with four diversity positions being divided among 120 mixtures, for a total diversity of 738,192 unique compounds.

Screening of positional scanning libraries

As mentioned above, each mixture of the positional scanning library can be screened individually to determine potent functionalities. The positional scanning mixtures in the TPI1346 library were screened in the excisive recombination pathway (see [1] for review). The mixtures with defined functionalities at the first three diversity positions (R^1 , R^2 and R^3) averaged 10–15% HJ accumulation at $1.0 \mu\text{g/mL}$ (ORs 7, 8, and 9). Mixtures with the following three functionalities exhibited a significant amount of HJ accumulation: the R and S isomers of 2-naphthylmethyl, and R-4-hydroxybenzyl. Although these mixtures accumulated a small fraction of substrates as HJs at $1.0 \mu\text{g/mL}$, they outperformed all others at $0.5 \mu\text{g/mL}$. (Note: This observation is similar to the case of peptides KWWCRW and WRWYCR: very high concentrations of a compound may inhibit the first DNA cleavage step in the recombination reaction, thereby reducing the % HJ formed ([31], data not shown).) Mixtures with defined functionalities at the R^4 position were tested at $1 \mu\text{g/mL}$ (OR 10); on average, 9% of the starting substrates were accumulated as HJs. From these data, the defined functionalities 2-biphenyl-4-yl-ethyl and 3,4-dichlorophenylethyl were selected for incorporation at position R^4 (again, these functionalities outperformed all others at $0.5 \mu\text{g/mL}$). Finally, the functionality

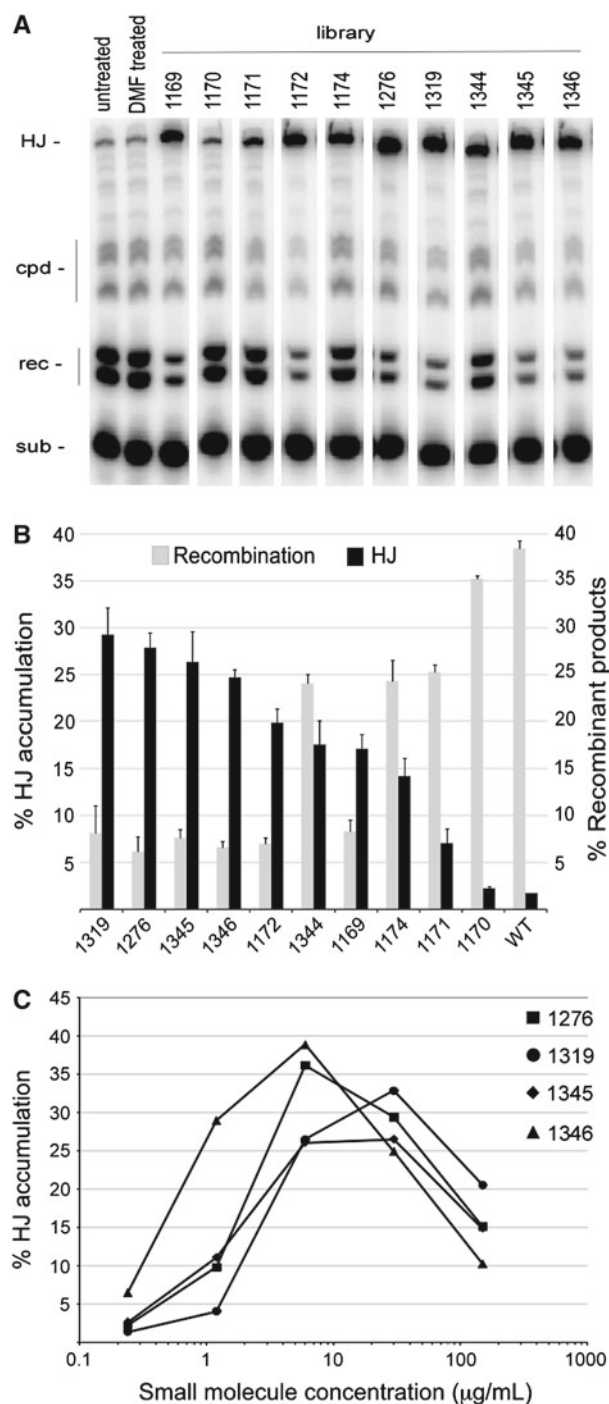


Fig. 3 Scaffold ranking. **a** Representative lanes from several gels showing the effects of inclusion of various small R group pools on bent-L recombination. Sub, radiolabeled substrate that recombines with an unlabeled partner site to produce recombinant products, “rec.”, “CPD,” covalent protein–DNA complexes; *HJ* Holliday junction. **b** Each mixture was tested at a concentration of $30 \mu\text{g/mL}$ and the average for all R group mixtures was determined. The error bars reflect the differences between R group pools within a given library. **c** Performance of the four most potent scaffolds evaluated by extent of HJ accumulation and IC_{50} values for recombination. High concentrations also inhibit the first cleavage event, reducing the HJ formed (refer to the mechanism of λ -SSR shown in Fig. 1a)

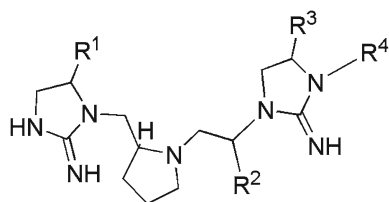


Fig. 4 Pyrrolidine bis-cyclic guanidine scaffold, library TPI1346

2-adamantan-1-yl-ethyl was included because of its non-aromatic ring-like structure, to examine the effect of size/shape at this R position (“Discussion” section). The functionalities selected for synthesis of individual compounds are marked with an asterisk in ORs 7–10, and yielded 36 possible individual combinations ($R^1 = 2$, $R^2 = 2$, $R^3 = 3$ and $R^4 = 3$, $2 * 2 * 3 * 3 = 36$, OR 11).

Synthesis of individual compounds

Compounds were synthesized as described previously [24], and individual compounds were designated 1609-1 through 1609-36. After synthesis and cleavage from solid-phase support, compounds were resuspended in 50% DMSO and analyzed by liquid chromatography-mass spectrometry (LC-MS) and determined to be 70–80% pure. In order to select candidates for purification, these compounds were then screened in the following assays: accumulation of HJs and inhibition of excision reactions (OR 12), binding to protein-free HJs (OR 2), non-specific linear DNA binding (data not shown), inhibition of the HJ resolvase complex RuvABC (OR 12), hemolytic activity (OR 13), and inhibition of bacterial growth (data not shown). We also used these data to preliminarily assess the role of R group stereochemistry on selected parts of the scaffold (OR 14). The results of these assays were used to select four compounds for purification and characterization.

Compound characterization

Compounds 1609-1, 1609-3, 1609-10, and 1609-12 (Fig. 5) were purified, and their masses were confirmed by high-resolution mass spectrometry (OR 1).

The four compounds were titrated in excisive recombination reactions and shown to be inhibitory in a dose-dependent manner (Fig. 6a). Inhibition of recombination was quantified at seven concentrations (0.25–8 $\mu\text{g}/\text{mL}$), and those data were used to estimate the IC_{50} values shown in Table 1. For comparison, the IC_{50} values of the peptides and the previously identified *N*-methyl aminocyclic thiourea [26] inhibitor 1530-1 are listed.

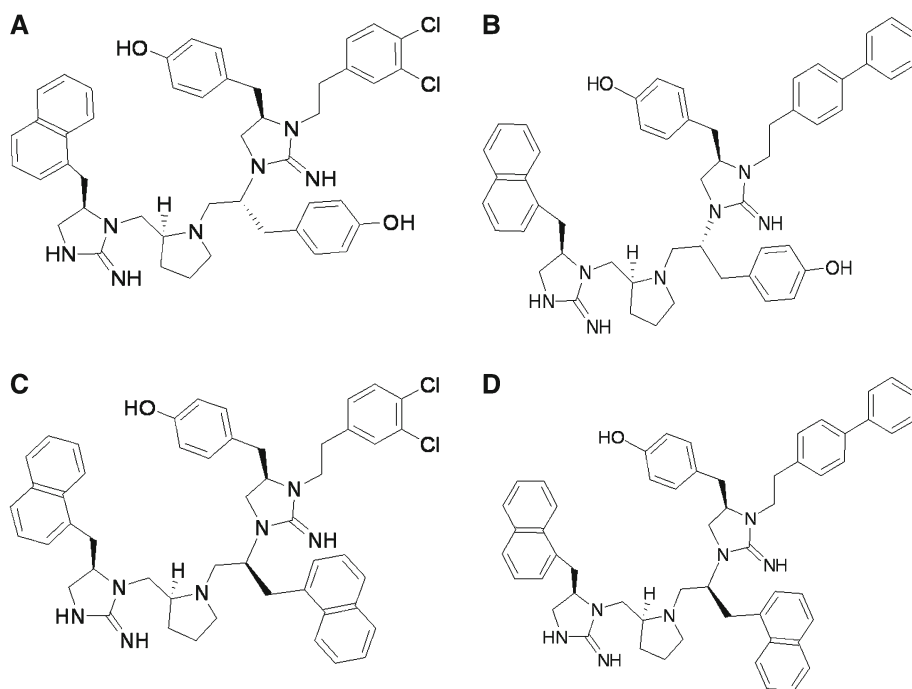
The HJs arise in multiple pathways in vivo, and are acted upon by several proteins/complexes with distinct mechanisms and structures. To determine whether other HJ-pro-

cessing enzymes are inhibited by the compounds, we tested their effect on the activity of the *E. coli* RecG protein. This monomeric helicase is conserved across almost all the bacterial species and functions in recombination-dependent DNA repair by unwinding a variety of branched DNA substrates to prevent the so-called pathologic replication (reviewed in [32]). In vitro, the purified enzyme converts a single HJ to two partial DNA duplexes in the presence of ATP and magnesium [9,33]. We tested the ability of the four selected compounds to interfere with RecG helicase (Fig. 6b) and found dose-dependent inhibition of unwinding activity. Based on these titrations, we estimated the IC_{50} values for each compound, and the results are shown in Table 1.

In order to address the specificity of these compounds for other DNA modification reactions, we assayed their effects on DNA cleavage by the *Hind*III restriction enzyme at the single recognition sequence in pUC19 plasmid DNA. Reactions were treated with each of the four selected compounds at a concentration near the IC_{50} values for recombination and HJ unwinding (1 $\mu\text{g}/\text{mL}$), and at a 10-fold higher concentration (10 $\mu\text{g}/\text{mL}$). Aliquots were removed from reactions at various time points, quenched with SDS, and electrophoresed on agarose gels to quantify the extent of DNA restriction over time (data not shown). Restriction inhibition values in the presence of the DMSO solvent were subtracted from restriction inhibition values of reactions treated with each small molecule, to obtain the corrected reaction velocities. The data in Table 1 are listed as the corrected % DNA restriction/min with respect to untreated reactions. As seen, none of the compounds affected DNA restriction by *Hind*III at 1 $\mu\text{g}/\text{mL}$, while some did inhibit, by as much as ~90%, at 10 $\mu\text{g}/\text{mL}$; this suggests that the 1609 compounds have less specificity for the HJ substrate than the peptides or compound 1530-1, but still prefer HJ substrates over B-form double-stranded DNA.

To further examine the nature of the interactions between the small molecules and the HJ, we tested whether 1609-10 could recognize protein-free HJs in an EMSA. This assay measures the ability of the compound to bind to and change the conformation of a synthetic HJ (Fig. 6c). In solution, HJs isomerize between “stacked-X” and “open square” conformations; in the former having more compact conformation, the arms of the junction fold in such a way that the center of the junction is occluded, whereas in the open with more extended conformation, the junction center is accessible to solvent [15,35]. Under some conditions, junctions can take on either the open or the stacked form; in the leftmost lane of Fig. 6c, the junction is seen as an unequal mixture of the two conformations. Adding 1609-10 to it changes the conformation of the junction into the open form in a dose-dependent manner; this band shift is similar to that seen with the peptides [9] and 1530-1 [36]. We hypothesized that this shift results from 1609-10 binding at the center of the HJ.

Fig. 5 Compounds selected for purification. Shown are compounds **a** 1609-1 (M.W. 804.85 g/mol), **b** 1609-3 (M.W. 812.05 g/mol), **c** 1609-10 (M.W. 838.91 g/mol), and **d** 1609-12 (M.W. 846.11 g/mol)



To test this hypothesis, we used a 2-AP fluorescence-quenching assay; this assay was used previously to determine the binding affinity of peptide WRWYCR to several branched DNA substrates, including HJs [6,37,38]. In brief, synthetic HJs were assembled using oligonucleotides where a single adenine was substituted with its fluorescent analog 2-AP at the center of the HJ substrate. In dsDNA, the fluorescence of 2-AP is quenched by base stacking with flanking bases. The 2-AP residue at the center of the junction has no stacking neighbor on one side and thus displays about half the maximal fluorescence compared to that seen in single stranded DNA [38]. This fluorescence may be quenched by the binding of an inhibitor at the center of the junction, as seen for the peptides [6].

Earlier, we found that the position of the 2-AP reporter around the HJ branch point influenced the strength of the fluorescence signal [6]. Therefore, we measured binding to a HJ substituted with 2-AP at a single position that consistently gave a strong signal (position 4AP2, OR 2A). We performed three independent titrations with 15–20 concentrations of 1609-10 ranging from 0 to 900 nM. We performed similar titrations on a junction without the 2-AP substitution to correct for the background fluorescence of dsDNA ($F_{\text{corr}} = 2\text{-AP substrate} - \text{noAP substrate}$ at all small molecule concentrations). F_{corr} values for each titration were used to calculate the fraction of HJ in a complex with 1609-10 (fraction of complex) using the equation found in the “Experimental section”. We compared this experimentally determined curve with predicted binding curves that were generated, based on six different scenarios to describe the interactions between

1609-10 and the HJ (these models (A–F) are discussed in detail in OR 3). In brief, in model A, we considered the binding of a single small molecule as a monomer to the HJ (designated L for ligand and R for receptor, both here and in OR 3). We next considered a nearly simultaneous three-body collision between R and two molecules of L to form an $R(L)_2$ complex (Model B). The third model considered the possibility that the small molecule first dimerizes to form L_2 and that this dimer then competes with the binding of a monomer to the junction; in this case, the only form active for binding is the monomeric form of L (Model C). Alternatively, the fourth model considered only the dimerized L_2 as the active species for binding (Model D). The fifth model considered the successive binding of two monomers to the junction, creating first a RL complex and then a $R(L)_2$ complex (Model E), while the sixth model described the same scenario with the additional possibility of L_2 formation (Model F). We ranked the models based on the smallest value of sum-squared error between the predicted and the observed curves (Fig. 7a) and on the lowest Akaike Information Constant (AIC), which also considers the number of variables and “favors” the best model with the fewest variables (OR 3). The analysis showed that model E was superior to the others in describing the observed data, as it has both the smallest AIC value and the lowest sum-squared error. The modeling predicted that the dominant form of the HJ complex in solution contains at least two ligands (Fig. 7b); even at low concentrations of 1609-10, there is not much RL complex present. The apparent binding constant (K_d , defined as the [1609-10] which supports conversion of 50% substrate into a HJ-small molecule complex) is

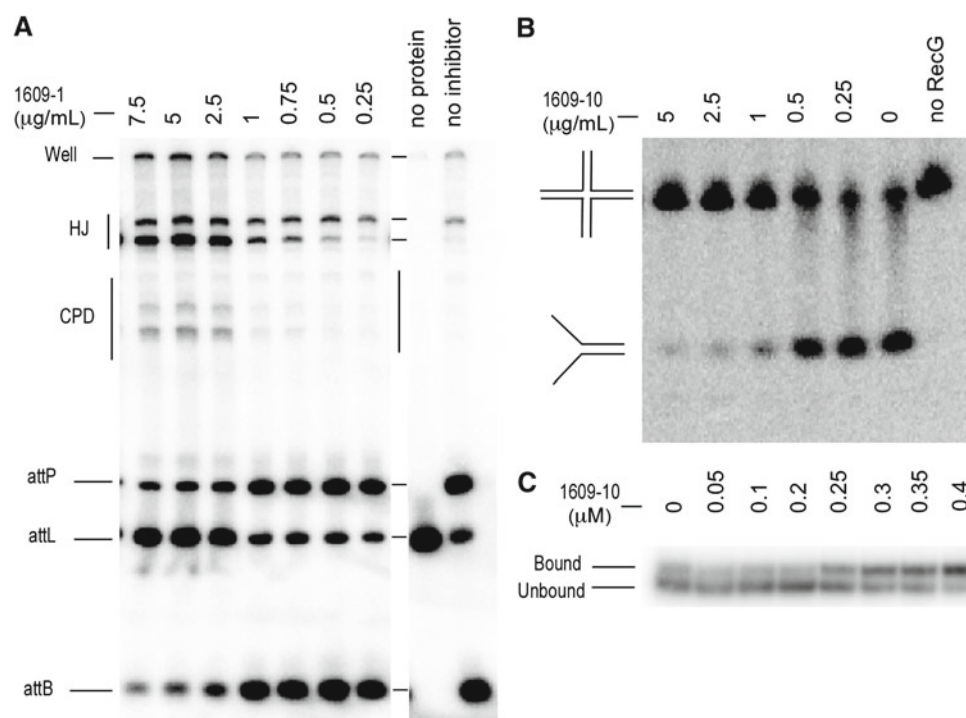


Fig. 6 Small molecules interact with HJs. **a** Slices from a representative SDS–tricine gel showing a dose titration of 1609-1 into an excision reaction. Recombination proteins (Int, IHF, and Xis) recombine a radiolabeled substrate, *attL*, with an unlabeled partner site, *attR*, to form the recombinant products *attP* and *attB*. The HJ intermediate of this reaction is stabilized by 1609-1, blocking progression to products or regression to substrates (see Fig. 1a). CPD, covalent protein–DNA complex; the lower HJ band is free HJ, while the upper HJ band is incompletely ligated, with Int still covalently attached. **b** An example of a HJ unwinding assay catalyzed by the RecG helicase. In the presence of HJ DNA, ATP and Mg^{+2} , RecG unwinds the HJ into two partial DNA duplex mol-

ecules, and this activity is inhibited by 1609-10 in a dose-dependent manner. IC_{50} values determined for 1609-1, -3, -10, and -12 for both excision and HJ unwinding were averaged from multiple titrations and are listed in Table 1. **c** 1609-10 binds to HJ. Radioactive end-labeled HJs run predominantly as a faster migrating unbound species in the absence of 1609-10. Treatment with increasing amounts of 1609-10 leads to a shift to a slower conformation. In some ionic conditions, we see a mixture of the two conformations (see text). The 1609-10-dependent transitions are not seen with DMSO alone. The estimated K_d for this binding reaction is ~ 300 nM

Table 1 Summary of in vitro activities of selected inhibitors

Compound	Molecular weight (g/mol) ^a	HJ binding (K_d)		DNA repair (μ g/mL) IC ₅₀ RecG	Recombination (μ g/mL) IC ₅₀ excision	% DNA restriction by <i>HindIII</i> ^b	
		2-AP	EMSA			1 μ g/mL	10 μ g/mL
WKHYNY	910.1	None	No shift	91.01 ^c	18.2 ^c	NT	NT
WRWYCR	1936.2	14 nM ^d	12.5 nM ^e	0.16 ^c	0.04 ^c	100 ^f	100 ^f
1530-1	423.5	NT	11.8 μ M ^g	0.36	10.5	100 ^g	100 ^g
1609-1	804.85	NT	NT	1.92	1.2	100	79
1609-3	812.05	NT	NT	1.18	1.2	100	54
1609-10	838.91	250 nM	300 nM	0.94	1.8	100	39
1609-12	846.11	NT	NT	0.75	0.7	100	11

NT not tested, None no binding detected in the 2-AP assay [6]

^a Molecular weight of active species; in the case of WRWYCR, this is a dimer

^b Numbers listed are the % activity at the indicated inhibitor concentration (corrected for DMSO effect) compared to untreated reactions

^{c,d,e,f,g} Numbers listed are from Refs. [8,6,9,4,34], respectively

^{f,g} Reactions treated with 100 μ g/mL compound, the maximum concentration tested, showed no inhibition of DNA restriction by the enzyme *HindIII*

approximately 250 nM (Table 1). This binding constant is in good agreement with that derived from the gel-based EMSA shown in Fig. 6c (K_d of ~ 300 nM, Table 1). Together these data indicate that 1609-10 has significantly lower affinity for the HJ compared to peptides WRWYCR or KWWCRW; however, it has almost 50-fold greater affinity for the HJ than the previously identified small molecule, 1530-1.

Homodimers of WRWYCR and KWWCRW are predicted to carry a +4 charge at the pH of our binding assays, and are significantly more basic than the four 1609 compounds. This difference in charge may affect both the affinity of the compounds for the HJ and the stability of their interactions with the HJs. In order to address this possibility, we performed dilution assays of HJ resolution reactions treated with 1609-10 and measured HJ resolution over time. In brief, we assembled purified protein-free lambda excision HJ substrates first with the inhibitory molecule and then added Int, IHF, and Xis. These reactions were incubated for 30 min to reach equilibrium, and then diluted 20-fold with buffer containing 2 μ g nonspecific DNA and a 28-fold molar excess of unlabeled HJ. If the inhibitor was bound stably to the excision HJ substrate, like WRWYCR, then this interaction should resist dilution; however, if the interaction is weak and short-lived, then the inhibitor should dissociate from the radioactively end-labeled junctions, rebinding most likely to the unlabeled junctions and allowing the stably bound recombination proteins to resolve the labeled HJ to products [4]. Figure 8a is representative of several experiments testing different concentrations of 1609-10 or WRWYCR. For each experiment, undiluted reactions and reactions assembled in the final dilute volume provided an indication of the level of inhibition at a given volume and concentration of inhibitor. As seen from the 10 μ L reaction controls, inhibitors are present in high enough concentrations to be effective during the initial 30-min incubation (compared to untreated with each inhibitor treatment). The 200- μ L reactions show little HJ resolution, indicating that the recombination proteins are not present at high enough concentrations to perform efficient catalysis; therefore, the resolution seen in the 10 \rightarrow 200 treatments is due to stably bound Int, Xis, and IHF. Regardless of the concentrations of inhibitors used, reactions treated with WRWYCR consistently showed 3–5-fold less HJ resolution (measured as % HJ resolution/min using a linear trendline) than reactions treated with 1609-10 (Fig. 8b). This indicated that 1609-10 binds to HJs less stably than peptide WRWYCR.

Inhibition of bacterial growth

The ability of the four selected compounds to inhibit the growth of several bacteria was assayed using the standard broth microdilution MIC assay method [28]. The Gram-neg-

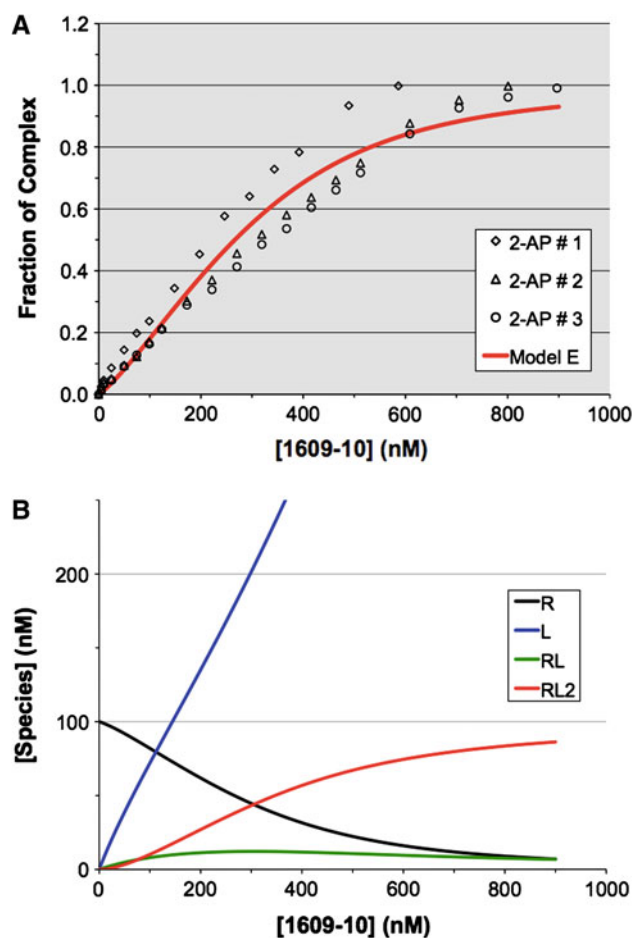


Fig. 7 **a** Fraction of HJ in a complex with 1609-10. Three independent titrations of the fluorescent reporter substrate HJ4AP2 (100 nM, see OR 2A) with 1609-10 were performed. The average fluorescence was measured, as described in the “Experimental section”, following 3 min of gentle stirring to allow complex formation for each successive addition of 1609-10. Similar titrations were performed on a HJ without the 2-AP base, and these fluorescence data were subtracted from the HJ4AP2 measurements to obtain values corrected for the background fluorescence of dsDNA and small molecule. The corrected values were then used to calculate the fraction of HJ in a complex with 1609-10 (fraction of complex), as described in the text. The three datasets are shown above as *open markers*; the *uninterrupted line* in the figure represents the predicted fraction of complex formed based on a model where the HJ can accommodate one or two 1609-10 molecules binding successively (see OR 3 model E, for further description of the mathematical modeling). **b** Predicted concentrations of each molecular species in solution calculated based on model E. All species present in the binding reaction, namely, the HJ (R or Receptor), 1609-10 (L or Ligand), and the complex with either 1 or 2 molecules of 1609-10 (RL or R(L)₂), respectively) are plotted with respect to the amount of 1609-10. As the amount of 1609-10 is increased, RL and R(L)₂ form, with R(L)₂ quickly becoming the dominant complex in solution. The plotted values for L are the amounts of unbound L in solution

ative bacteria used were *E. coli* K12, *Salmonella enterica* serovar Typhimurium (STm), and a hyperpermeable STm *galE rfa* mutant with short LPS chains; the Gram-positive bacteria used were *B. subtilis* and methicillin-resistant

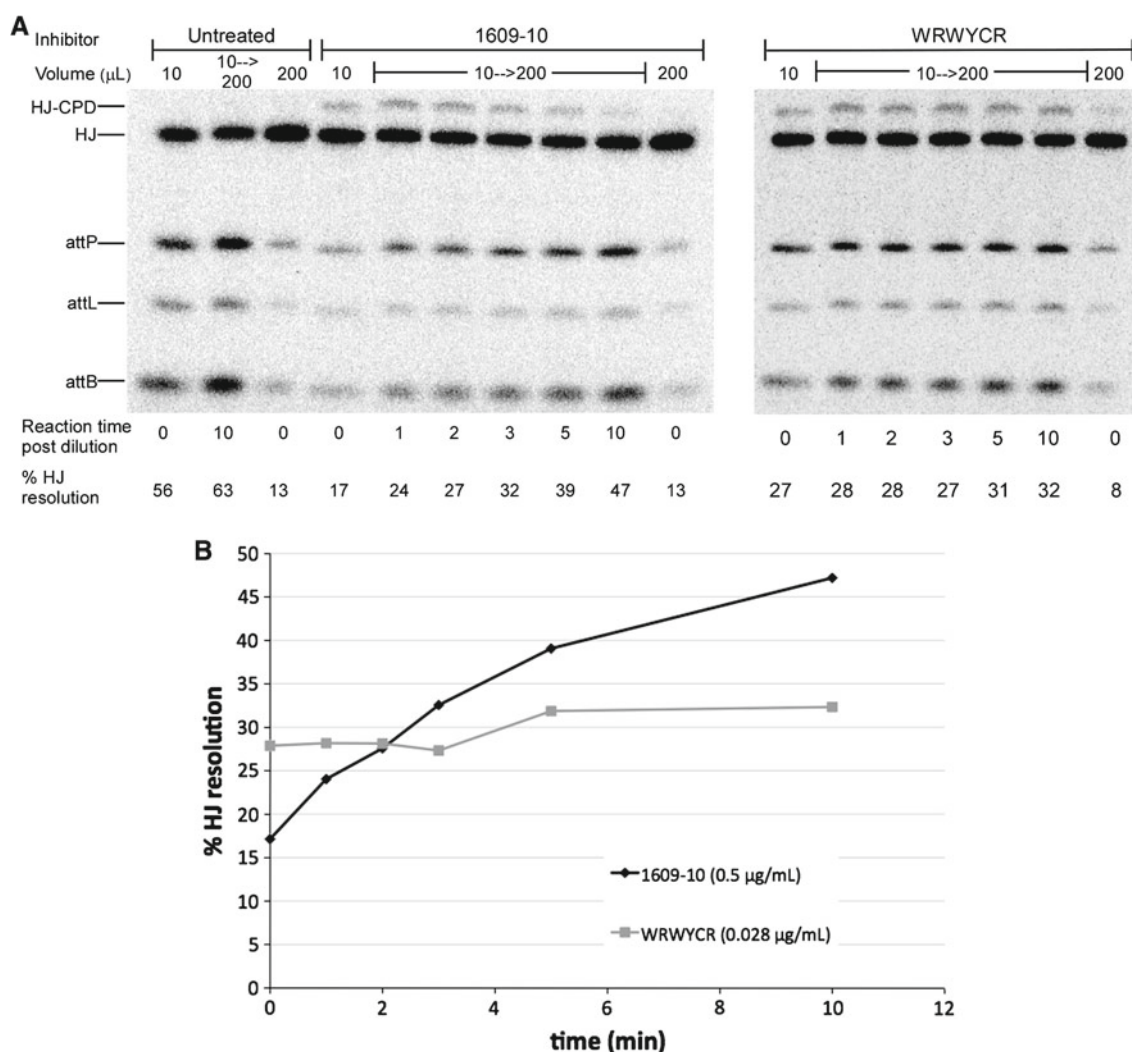


Fig. 8 HJ resolution assay to examine the stability of interactions between inhibitors and the HJ. **a** Excision HJs (20 pM) were incubated with recombination proteins in the presence or the absence of inhibitors for 30 min. After initial incubation, reactions were either stopped with SDS (controls), or diluted 20-fold with 2 μg nonspecific DNA, and a 28-fold molar excess of unlabeled HJ over each inhibitor (shown as

10 \rightarrow 200). Reactions were stopped at various time points, as shown, and loaded on SDS–tris–tricine gels to separate the HJ from the recombinant products (*attP*, *attL*, and *attB*). HJ–CPD refers to a sub-population of HJs with an Int molecule covalently bound to the DNA. **b** Graph of the % HJ resolution/min, beginning after dilution of the initial reaction

S. aureus (MRSA). As seen in Table 2, the four selected compounds have a wide range of MIC values against the various bacteria tested, but were generally more potent against Gram-positive bacteria than against Gram-negative bacteria. This is probably due to the outer membrane LPS on Gram-negative bacteria, as indicated by the 2–16-fold greater sensitivity of the STm *galE rfa* mutant to the small molecules compared to STm LT2. It was notable that, unlike the previously identified small molecule 1530-1, selected 1609 compounds are also effective against the wild-type LT2 strain. Moreover, the most potent of the 1609 compounds

had lower MICs than the peptides against all of the bacteria tested.

Eukaryotic cell toxicity

Three of the four selected compounds were tested for their effect on viability and metabolic activity of eukaryotic cells using an MTT assay. This assay relies on the activity of reductases in healthy mitochondria to convert MTT to a purple formazan, which can be measured spectroscopically [39]. As seen in Fig. 9, the 1609 compounds do inhibit eukaryotic

Table 2 MICs ($\mu\text{g/mL}$) for selected compounds

Compound	Strain				
	<i>E. coli</i> MG1655	<i>S. enterica</i> LT2	<i>S. enterica gal rfa</i>	<i>B. subtilis</i>	MRSA
1530-1	>100	>100	>100 ^a	>100	>100
1609-1	8–16	16	2–8	2	2
1609-3	8–16	16–32	2–4	2	2
1609-10	16	16–32	2–4	2–4	2
1609-12	32–64	32–64	2–4	2	2
wrwyrcr	32–64	32–64	16–64	8–16	16
Erythromycin	32–64	32–64	2–4	1	32–128

Each MIC value is the average of at least three independent experiments; in this table (in contrast to Table 1), the MIC values were calculated using the MW of monomer wrwyrcr

^a At 100 $\mu\text{g/mL}$, the final OD₆₀₀ of the *S. enterica* AMES strain was reduced by 50% compared to the wild-type *S. enterica* LT2 after 22 h of incubation at 37 °C

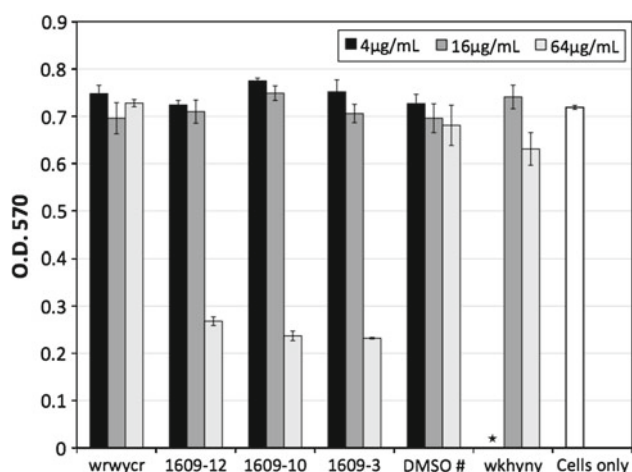


Fig. 9 MTT reduction assay. The effects of 1609-12, 1609-10, and 1609-3 were assayed for toxicity to BSC40 eukaryotic fibroblasts. Peptides wrwyrcr and wkhyrcr were also assayed, for comparison. Cells were grown in 96-well plates and treated with peptides or small molecules at the indicated concentrations for 24 h. After treatment, the cells were allowed up to 3 h to convert MTT to formazan, as measured by the optical density at 570 nm: higher OD values reflect higher viability and metabolic activity. The average OD₅₇₀ of the compounds is shown from three independent experiments. * 4 $\mu\text{g/mL}$ of wkhyrcr was not tested. DMSO #—the same DMSO solvent concentrations were used in these control reactions as those that were present in reactions treated with wrwyrcr

cells at 64 $\mu\text{g/mL}$ by about 65%, but not at 16 $\mu\text{g/mL}$ or lower.

Discussion

The aim of this study was to identify small molecule surrogates of peptide inhibitors that bind to HJ intermediates of SSR [4], inhibit DNA repair proteins, and have antibacterial properties. The small molecule libraries we screened

(OR 5) were specifically chosen to have some measure of twofold symmetry about the scaffold, in an effort to mimic the active dimer form of the most potent hexapeptides (for example, see WRWYCR, Fig. 1b). Support for this reasoning comes from structure–activity relationship (SAR) studies of WRWYCR using alanine scan mutagenesis, which showed that some symmetry within the active peptide is important for interactions with HJs and for antimicrobial activity [6,9] (A. Flores-Fujimoto and A. M. Segall, unpublished data). In fact, dimerization of WRWYCR is necessary for inhibition of recombinases and HJ-processing enzymes [4,9], as well as for bacterial growth inhibition [8]. Further support comes from the crystal structure of a complex between Cre recombinase and the HJ intermediate trapped by peptide WKHYNY (Fig. 1c), which strongly suggests that two monomer peptides per complex are necessary for binding and inhibition of enzyme activity [37]. We presume that the need for symmetry stems from the fact that these inhibitors bind to a target with a pseudo twofold axis of symmetry [35], and thus we searched for small molecule scaffolds that could accommodate this characteristic.

The positional scanning data used to identify all inhibitors [2–4,12,36] showed that there are common functionalities that correlate well with efficacy, both in vivo and in vitro: specifically, the most potent molecules are those with aromatic functionalities, basic functionalities, and groups capable of forming hydrogen bonds. In silico molecular modeling, corroborated by fluorescence quenching studies, suggests that the aromatic functionalities on peptide WRWYCR are necessary for interactions with HJs and are likely to establish orthogonal and/or planar π – π interactions with solvent-accessible bases at the center of the HJ [6] (R. Saha and A. M. Segall, unpublished data). The aromatic functionalities 2-naphthylmethyl and 4-hydroxybenzyl, identified as necessary for effective inhibition of SSR in the 1609 set of small molecules, are also likely to establish base stacking

interactions with the HJ DNA. Aromatic functionalities are present at all the three diversity positions in the most potent mixtures, suggesting that the nature of the functional group rather than its specific placement on the scaffold is the dominant aspect affecting compound activity. Further, this suggests that given an appropriately flexible scaffold, the functionalities may be able to adopt several effective conformations. Along these lines, macrocyclic peptide analogs that were specifically designed to be less flexible are only moderately effective at binding HJs and were ineffective at inhibiting bacterial growth [40,41] despite having aromatic functionalities of a similar nature as linear peptides or the 1609 compounds. Aromatic functional groups also ranked high at position R⁴ in terms of inhibition of SSR. We used this position to test whether shape and/or hydrophobicity of the functionality would more highly impact interactions with HJs by incorporating the large hydrophobic but aliphatic functionality 2-adamantan-1-yl-ethyl (OR 11) derived from 1-adamantaneacetic acid (OR 6). However, compounds containing this functionality performed poorly in most of our assays despite a high ranking in the positional scanning (OR 10). This could be viewed as further support for the importance of aromatic functionalities in the inhibitors. Alternatively, this functionality may be potent only in combination with R-group functionalities that were present in the mixtures but were not selected for individual compound synthesis.

Positional scanning identified basic functionalities in all of the peptides and the 1530 set of small molecules [36]. These groups are likely to be protonated at the pH of our in vitro reactions as well as inside cells, which may facilitate inhibitor binding to negatively charged DNA. These basic functionalities, usually derived from lysine, arginine, or following methylation and reduction of glutamine (1530-1, position R¹), were not present in small molecule library TPI1346, to avoid complications with the cyclization step used to generate the bis-cyclic guanidine groups. The SAR studies of peptide WRWYCR suggested that the arginine residues, particularly the one at the 6th position, are very important for SSR inhibition and protein-free HJ binding (A. Flores-Fujimoto et al., unpublished data). While it is possible that the guanidine groups on the scaffold may be protonated, their charges may not be close enough to the DNA to make efficient ionic interactions. Thus, the decrease in the number of flexible, basic functionalities between WRWYCR and 1609-10 may have caused, at least in part, the observed decrease in the affinity and stability of binding interactions with HJ DNA.

Finally, the positional scanning data suggested that functional groups capable of forming strong hydrogen bonds contribute to the potency of these inhibitors with regard to inhibition of SSR and the other in vitro activities of these small molecules. Modeling of WRWYCR suggested that hydrogen bond interactions, especially those along the amide backbone, probably contribute to the stabilizing interactions

between the peptide inhibitors and the HJ substrate [6]. While it is difficult to predict where hydrogen bonds will form, 1530-1 has far fewer electrophilic atoms capable of forming hydrogen bonds than the peptides, and the 1609 set of small molecules has only the phenolic groups of 4-hydroxybenzyl at positions R² and R³. This functionality, derived from tyrosine, has performed well in all our screens and was also a determining factor in the activity seen with the macrocyclic peptide inhibitors [40]. Thus, the absence of strong hydrogen-bonding potential probably contributes to the decrease in stability/affinity of the 1609 compounds with HJ substrates and may also contribute to the increase in IC₅₀ for SSR with respect to the peptides wrwycr and kwrcrw. While this increase is unfavorable, fewer hydrogen bond donor/acceptors are generally considered better in terms of therapeutic potential [20,21] and the 1609 set of small molecules has far fewer of these electrophilic species than the peptides.

The results of this study showed that binding to protein-free HJs is not necessarily indicative of inhibitory activity in our enzyme assays involving HJs. For instance, 1609-10 has nearly 50-fold greater affinity for protein-free HJs than 1530-1 ($K_d = 0.25\text{--}0.3\mu\text{M}$ vs. $11.8\mu\text{M}$, respectively; Table 1); yet both inhibitors are equally potent at inhibiting RecG-mediated HJ unwinding (Table 1) and are within 10-fold of potency compared with the active peptides. RecG interacts with HJ as a monomer, and has low processivity [33,42], factors which probably make it prone to being easily inhibited. In contrast, the compounds we have identified to date have a wide, 500-fold range of potencies at inhibiting excisive recombination, indicating that this reaction provides better discrimination of inhibitor efficacy. We note that, while 1530-1 inhibits excision reactions fivefold more poorly compared to 1609-10, the former compound was identified using bent-L recombination assays and is about fivefold more potent in those reactions than in excision reactions [34]. Differences in the architecture of the HJ intermediates in those recombination reactions may account for the different potencies seen (discussed in Ref. [2]).

We used the 2-AP fluorescence quenching data to test several possible models of 1609-10 binding to a HJ (OR 3). The best curve fit came from a model where 1609-10 binds to a HJ first as monomer, but allows enough space for a 2nd molecule to bind subsequently. Several of the models tested the possibility of a dimer of 1609-10 forming in solution, but in every case, the equilibrium constant for dimer formation was so low that we deem this scenario unlikely. Furthermore, we have no evidence of dimer formation from HPLC analysis of 1609-10 solutions. Therefore, the equilibrium state of this complex may be similar to that suggested by the crystal structure of the less-active monomeric peptide inhibitor WKHNY bound to a HJ, where two molecules bind in discrete corners of the junction, but are not physically connected to each other [37]. We also tested models that predicted one

molecule of 1609-10 binding and forming a saturated complex, but these also did not fit the data well, further supporting the hypothesis that at least two molecules bind the HJ. These results imply that we may have isolated a more active surrogate of the monomer peptide that still does not make sufficient contacts with the HJ substrate to provide the affinity or the stable interactions characteristic of the dimerized peptide WRWYCR. With this in mind, we will include a sulfhydryl functionality in future small molecules to facilitate their dimerization, and test whether their potency increases concomitantly. A caveat is that our modeling analysis does not exclude the possibility that more than two molecules bind to the HJ either at the center or on the arms, in a non-specific manner. In fact, the 1609 set of compounds appear to be less specific for HJs than other inhibitors that we have identified to date. This is evident from their inhibition of DNA restriction enzymes (whose structure, mechanism of catalysis, and interaction with DNA differ fundamentally from those of the tyrosine recombinases) and further supported by band shifts of linear double-stranded DNA conducted with the crude compounds where, at 10 $\mu\text{g/mL}$, the small molecules caused non-specific shifts of the DNA into the wells of the gel [31]. Furthermore, our modeling studies also do not exclude the possibility of non-equivalent binding sites for these molecules, a scenario that seems likely since the DNA sequence is not identical on all the corners of the junction center. Atomic level structural data will resolve these questions, and X-ray crystallography studies are in progress.

The 1609 compounds inhibited bacterial growth, particularly in the case of Gram-positive strains with MICs in the 2–4 $\mu\text{g/mL}$ range, and surpassed the potency of the peptides even in Gram-negative bacteria. Experiments with a *Salmonella* hyperpermeable mutant indicated that the compounds have greater difficulty passing through the outer membrane of Gram-negative bacteria. The greater antimicrobial activity of these compounds was surprising given that these compounds were less potent inhibitors of recombination. While the 1609 compounds clearly interact with HJs and interfere with HJ processing enzymes, it is possible either that they enter bacterial cells more readily than the peptides, and/or that they have additional targets in vivo. Further characterization of the effects of the bis-cyclic guanidine inhibitors on microbial physiology suggests that they induce envelope stress in bacteria, in addition to potentially interfering with DNA repair (S. Yitzhaki et al., data not shown). The 1609 compounds described are very hydrophobic, and we have obtained evidence that their toxicity may be due at least in part to some membrane perturbations. On-going compound syntheses aimed at optimizing the charged functionalities by including more polar groups may help alleviate this phenotype. Results from our hemolysis studies showed that the presence of R-4-hydroxybenzyl at position R³ is correlated with lower hemolysis (J. L. Boldt et al., data not shown),

whereas compounds containing either the R or S isomers of 2-naphthylmethyl at position R³ were more hemolytic. This trend was not seen at position R² when 4-hydroxybenzyl was compared with 2-naphthylmethyl.

In summary, we have now identified a second class of small molecules with the ability to block SSR- and HJ-processing enzymes in vitro; this set of molecules has much greater antimicrobial activity than 1530-1. While these compounds have good affinity toward HJs, they bind less stably to HJs than the previously identified peptide inhibitors. These compounds are the most potent inhibitors of bacterial growth that we have isolated to date using the HJ-trapping assay, perhaps due to greater permeability of the compounds. Our data suggested that modifications such as adding symmetry and/or aromatic functionalities to the 1530 series of compounds might dramatically improve their efficacy. Conversely, adding basic functionalities to the 1609 compounds may increase the stability of HJ binding, and perhaps decrease their toxicity. This new class of compounds may be a useful new addition to the current arsenal of antibiotics or disinfectants, particularly in an age of rising drug resistance.

Acknowledgments The authors gratefully acknowledge the expert technical help provided by Claudia Vallejo who performed the eukaryotic MTT studies, and the help provided by Rod Santos during the synthesis of the 36 individual pyrrolidine bis-cyclic guanidines. This study was supported as follows: by Public Health Service grants, RO1 GM052847 from the National Institute of General Medical Services and RO1 AI058253 from the National Institute of Allergy and Infectious Disease to AMS; by the National Science Foundation grant, 0827278, in part to GVF and PS; by Interdisciplinary Training in Biology and Mathematics grant to AMS and PS; by the State of Florida, Executive Office of the Governor's Office of Tourism, Trade, and Economic Development to AN and MG; and by the Multiple Sclerosis National Research Institute to JO and CP. MCR is the recipient of an Achievement Rewards for College Scientists scholarship.

References

1. Azaro M, Landy A (2002) λ Integrase and the λ Int family. In: Craig NL et al (ed) Mobile DNA II. ASM Press, Washington, DC, pp 118–149
2. Cassell G, Klemm M, Pinilla C, Segall A (2000) Dissection of bacteriophage lambda site-specific recombination using synthetic peptide combinatorial libraries. *J Mol Biol* 299:1193–1202. doi:10.1006/jmbi.2000.3828
3. Klemm M, Cheng C, Cassell G, Shuman S, Segall AM (2000) Peptide inhibitors of DNA cleavage by tyrosine recombinases and topoisomerases. *J Mol Biol* 299:1203–1216. doi:10.1006/jmbi.2000.3829
4. Boldt JL, Pinilla C, Segall AM (2004) Reversible inhibitors of lambda integrase-mediated recombination efficiently trap Holliday junction intermediates and form the basis of a novel assay for junction resolution. *J Biol Chem* 279:3472–3483. doi:10.1074/jbc.M309361200
5. Cassell GD, Segall AM (2003) Mechanism of inhibition of site-specific recombination by the Holliday junction-trapping pep-

- tide WKHYNY: insights into phage lambda integrase-mediated strand exchange. *J Mol Biol* 327:413–429. doi:10.1016/S0022-2836(03)00058-5
6. Kepple KV, Patel N, Salamon P, Segall AM (2008) Interactions between branched DNAs and peptide inhibitors of DNA repair. *Nucl Acids Res* 36:5319–5334. doi:10.1093/nar/gkn512
 7. Gunderson CW, Boldt JL, Authement RN, Segall AM (2009) Peptide wrwyer inhibits the excision of several prophages and traps Holliday junctions inside bacteria. *J Bacteriol* 191:2169–2176. doi:10.1128/JB.01559-08
 8. Gunderson CW, Segall AM (2006) DNA repair, a novel antibacterial target: Holliday junction-trapping peptides induce DNA damage and chromosome segregation defects. *Mol Microbiol* 59:1129–1148. doi:10.1111/j.1365-2958.2005.05009.x
 9. Kepple KV, Boldt JL, Segall AM (2005) Holliday junction-binding peptides inhibit distinct junction-processing enzymes. *Proc Natl Acad Sci USA* 102:6867–6872. doi:10.1073/pnas.0409496102
 10. Segall AM, Nash HA (1996) Architectural flexibility in lambda site-specific recombination: three alternate conformations channel the *attL* site into three distinct pathways. *Genes Cells* 1:453–463. doi:10.1046/j.1365-2443.1996.d01-254.x
 11. Grindley ND, Whiteson KL, Rice PA (2006) Mechanisms of site-specific recombination. *Annu Rev Biochem* 75:567–605. doi:10.1146/annurev.biochem.73.011303.073908
 12. Fujimoto DF, Pinilla C, Segall AM (2006) New peptide inhibitors of type IB topoisomerases: similarities and differences vis-à-vis inhibitors of tyrosine recombinases. *J Mol Biol* 363:891–907. doi:10.1016/j.jmb.2006.08.052
 13. Cheng C, Kussie P, Pavletich N, Shuman S (1998) Conservation of structure and mechanism between eukaryotic topoisomerase I and site-specific recombinases. *Cell* 92:841–850. doi:S0092-8674(00)81411-7
 14. Champoux JJ (2001) DNA topoisomerases: structure, function, and mechanism. *Annu Rev Biochem* 70:369–413. doi:10.1146/annurev.biochem.70.1.369
 15. Lilley DM (2008) Analysis of branched nucleic acid structure using comparative gel electrophoresis. *Q Rev Biophys* 41:1–39. doi:10.1017/S0033583508004678
 16. Michel B, Boubakri H, Baharoglu Z, LeMasson M, Lestini R (2007) Recombination proteins and rescue of arrested replication forks. *DNA Repair* 6:967–980. doi:10.1016/j.dnarep.2007.02.016
 17. Cano DA, Pucciarelli MG, Garcia-del Portillo F, Casades J (2002) Role of the RecBCD recombination pathway in *Salmonella* virulence. *J Bacteriol* 184:592–595. doi:10.1128/JB.184.2.592-595.2002
 18. Loughlin MF, Barnard FM, Jenkins D, Sharples GJ, Jenks PJ (2003) *Helicobacter pylori* mutants defective in RuvC Holliday junction resolvase display reduced macrophage survival and spontaneous clearance from the murine gastric mucosa. *Infect Immun* 71:2022–2031. doi:10.1128/IAI.71.4.2022-2031.2003
 19. Su LY, Willner DL, Segall AM (2010) An antimicrobial peptide that targets DNA repair intermediates in vitro inhibits *Salmonella* growth within murine macrophages. *Antimicrob Agents Chemother* 54:1888–1899. doi:10.1128/AAC.01610-09
 20. Lipinski CA, Lombardo F, Dominy BW, Feeney PJ (2001) Experimental and computational approaches to estimate solubility and permeability in drug discovery and development settings. *Adv Drug Deliv Rev* 46: 3–26
 21. Lipinski CA (2000) Drug-like properties and the causes of poor solubility and poor permeability. *J Pharmacol Toxicol Methods* 44: 235–249
 22. Pinilla C, Appel JR, Borrás E, Houghten RA (2003) Advances in the use of synthetic combinatorial chemistry: mixture-based libraries. *Nat Med* 9:118–122. doi:10.1038/nm0103-118
 23. Nefzi A, Ostresh JM, Giulianotti M, Houghten RA (1999) Solid-phase synthesis of trisubstituted 2-imidazolones and 2-imidazolindinethiones. *J Comb Chem* 1:195–198. doi:10.1021/cc980019m
 24. Hensler ME, Bernstein G, Nizet V, Nefzi A (2006) Pyrrolidine bicyclic guanidines with antimicrobial activity against drug-resistant Gram-positive pathogens identified from a mixture-based combinatorial library. *Bioorg Med Chem Lett* 16:5073–5079. doi:10.1016/j.bmcl.2006.07.037
 25. Houghten RA, Pinilla C, Appel JR, Blondelle SE, Dooley CT, Eichler J, Nefzi A, Ostresh JM (1999) Mixture-based synthetic combinatorial libraries. *J Med Chem* 42:3743–3778. doi:0.1021/jm990174v
 26. Ranjit DK, Rideout MC, Nefzi A, Ostresh JM, Pinilla C, Segall AM (2010) Small molecule functional analogs of peptides that inhibit lambda site-specific recombination and bind Holliday junctions. *Bioorg Med Chem Lett*. doi:10.1016/j.bmcl.2010.06.029
 27. Sambrook J, Russell DW (2001) *Molecular cloning: a laboratory manual*, 3rd edn. Cold Spring Harbor Laboratory Press, Cold Spring Harbor
 28. Ferraro MJ (2000) National committee for clinical laboratory standards methods for dilution antimicrobial susceptibility tests for bacteria that grow aerobically: approved standard. NCCLS, Wayne
 29. Pinilla C, Appel JR, Blanc P, Houghten RA (1992) Rapid identification of high affinity peptide ligands using positional scanning synthetic peptide combinatorial libraries. *Biotechniques* 13:901–905
 30. Houghten RA, Pinilla C, Giulianotti MA, Appel JR, Dooley CT, Nefzi A, Ostresh JM, Yu Y, Maggiora GM, Medina-Franco JL, Brunner D, Schneider J (2008) Strategies for the use of mixture-based synthetic combinatorial libraries: scaffold ranking, direct testing in vivo, and enhanced deconvolution by computational methods. *J Comb Chem* 10:3–19. doi:10.1021/cc7001205
 31. Boldt JL (2006) Second generation small molecule inhibitors of lambda recombination with enhanced antimicrobial activity. M.S. Thesis, San Diego State University
 32. Rudolph CJ, Upton AL, Briggs GS, Lloyd RG (2010) Is RecG a general guardian of the bacterial genome?. *DNA Repair* 9:210–223. doi:10.1016/j.dnarep.2009.12.014
 33. Whitby MC, Lloyd RG (1998) Targeting Holliday junctions by the RecG branch migration protein of *Escherichia coli*. *J Biol Chem* 273:19729–19739. doi:10.1074/jbc.273.31.19729
 34. Ranjit DK (2004) Small molecules that inhibit recombination and bacterial growth. Dissertation, San Diego State University
 35. McKinney SA, Declais AC, Lilley DM, Ha T (2003) Structural dynamics of individual Holliday junctions. *Nat Struct Biol* 10:93–97. doi:10.1038/nsb883
 36. Ranjit DK, Rideout MC, Nefzi A, Ostresh JM, Pinilla C, Segall AM (2010) Small molecule functional analogs of peptides that inhibit lambda site-specific recombination and bind Holliday junctions. *Bioorg Med Chem Lett* 20:4531–4534. doi:10.1016/j.bmcl.2010.06.029
 37. Ghosh K, Lau CK, Guo F, Segall AM, Van Duyne GD (2005) Peptide trapping of the Holliday junction intermediate in Cre-*loxP* site-specific recombination. *J Biol Chem* 280:8290–8299. doi:10.1074/jbc.M411668200
 38. Declais AC, Lilley DM (2000) Extensive central disruption of a four-way junction on binding Cce1 resolving enzyme. *J Mol Biol* 296:421–433. doi:10.1006/jmbi.1999.3479
 39. Mosmann T (1983) Rapid colorimetric assay for cellular growth and survival: application to proliferation and cytotoxicity assays. *J Immunol Methods* 65:55–63. doi:10.1016/0022-1759(83)90303-4
 40. Pan PS, Curtis FA, Carroll CL, Medina I, Liotta LA, Sharples GJ, McAlpine SR (2006) Novel antibiotics: C-2 symmetrical macrocycles inhibiting Holliday junction DNA binding by *E. coli* RuvC. *Bioorg Med Chem* 14:4731–4739. doi:10.1016/j.bmc.2006.03.028

41. Bolla ML, Azevedo EV, Smith JM, Taylor RE, Ranjit DK, Segall AM, McAlpine SR (2003) Novel antibiotics: macrocyclic peptides designed to trap Holliday junctions. *Org Lett* 5:109–112. doi:[10.1021/ol020204f](https://doi.org/10.1021/ol020204f)
42. Slocum SL, Buss JA, Kimura Y, Bianco PR (2007) Characterization of the ATPase activity of the *Escherichia coli* RecG protein reveals that the preferred cofactor is negatively supercoiled DNA. *J Mol Biol* 367:647–664. doi:[10.1016/j.jmb.2007.01.007](https://doi.org/10.1016/j.jmb.2007.01.007)